Chemical Engineering Science 285 (2024) 119554

Contents lists available at ScienceDirect

Chemical Engineering Science

journal homepage: www.elsevier.com/locate/ces

The effect of inert gases (Xe, Ar, Ne, He) on decomposition reactions of N_2O, CH_4 and CO_2 at high pressures

Y. Slotboom *, S.R.A. Kersten *

Sustainable Process Technology, Faculty of Science and Technology, University of Twente, PO Box 217, 7500 AE Enschede, the Netherlands

ARTICLE INFO

Keywords:
High pressure
Homogeneous
Gas phase
Kinetics
Noble gases
Compression

ABSTRACT

In a pulsed compression reactor (PCR) experiments were done with N_2O ($4\%_{mol}$), CH_4 ($1\%_{mol}$) and CO_2 ($2\%_{mol}$) diluted in the inert gases Xe, Ar, Ne and He. The mixtures were compressed up to 250 bar, reaching temperatures of up to 4000 K. At equal temperature, pressure and volume, significant differences (up to 20%) were measured in the conversion of the three species in different noble gases. The measurements with N_2O decomposition showed that the reaction is the fastest in the most heavy noble gas tested. The conversion decreased as the molar mass of the noble gas decreased. Likewise, methane pyrolysis was measured to be the fastest in xenon and slowed down in accordance with the mass of the inert molecule. A reverse trend was measured for the decomposition of CO_2 to CO and O·, which is explained by the dominant role of the reverse reaction. As a result, the CO_2 data is also explained by conversion rates that are higher in heavier gases. This paper provides a first attempt to understand the observed influence of the molar mass of the inert bathing gas on the reaction rate in the high pressure domain. A theory is proposed based on a Newtonian description of reactant activation by the inert bathing gas.

1. Introduction

During our research into the non-oxidative thermal coupling of methane in the pulsed compression reactor (PCR) (Slotboom and Kersten, 2023; Slotboom et al., 2021) it was observed that at high pressures (>10 bar) the decomposition rate depends on the inert gas. This was unexpected by us and it triggered a further investigation into the extent of this effect. For the low pressure domain, calculations and experimental data on the effect of the bathing gas on reaction rates are present in literature (Golden, 2008; Jasper and Miller, 2009, 2011; Matsugi, 2019; Troe and Ushakov, 2012) (see ahead). Data in the high pressure domain is scarce (Barnes et al., 1989; Nativel et al., 2019) and will also be discussed further on. Most commonly experiments are done in argon only or at a time scale of seconds (Barnes et al., 1989; Nativel et al., 2019). This is of importance, because the effect that was measured in this work seems to only be present during short residence times.

It is our hypothesis that the observed influence of the inert gas on the reaction rate finds its origin in the collision of a reactant with the inert gas. Hence, the inert gas is a bathing gas that activates a reactant. Lindemann was the first to describe the effect of the bathing gas on unimolecular reactions. The Lindemann-Hinshelwood mechanism is a well-known and easily interpretable theory. It uses the concept of an activated or excited molecule [A] after a collision with an inert [I] (Eq. (1)). At sufficient energy the activated molecule can decompose into the products (Eq. (2)).

$$A + I \rightleftarrows A^* + I \tag{1}$$

$$A^* \rightarrow B + C \tag{2}$$

$$\frac{d[A]}{dt} = -\frac{k_1 k_2 [A][I]}{k_{-1}[I] + k_2} \tag{3}$$

The dependence on the pressure is reflected in the concentration of the bathing gas ([I]), see Eq. (3). At high pressures however the concentration of the bathing gas becomes irrelevant and the rate determining step becomes the dissociation of the activated molecule itself (Eq. (2)). Other theories were proposed after Lindemann's, like the RRKM theory and the transition state theory. They all follow the same principle that at high pressures the dependency on the concentration of the bathing gas [I] becomes negligible.

Lindemann stated that unimolecular reactions exhibit first-order kinetics at high pressures. It was theorized that this behaviour is present because molecules that are activated by collisions need a certain amount of time before it can dissociate. At high pressures this is the rate limiting step and the rate of activation by collision versus deactivation

* Corresponding authors.
E-mail addresses: y.slotboom@utwente.nl (Y. Slotboom), s.r.a.kersten@utwente.nl (S.R.A. Kersten).

https://doi.org/10.1016/j.ces.2023.119554
Received 10 July 2023; Received in revised form 17 October 2023; Accepted 21 November 2023
Available online 27 November 2023

by collisions is very high. The amount of collisions is sufficient enough to reach an equilibrium distribution of activated molecules (Callear, 1983). With the data in this work the question arises: is this equilibrium distribution of collisions (Eq. (1)) the same for all bathing gases?

1.1. Reported calculations on the effect of the bathing gas

Classical trajectory calculations for multiple bathing gases were done recently by different authors (Jasper and Miller, 2009, 2011; Matsugi, 2019). These theoretical models are verified on experimental data (Barnes et al., 1989; Baulch et al., 1992; Hidaka et al., 1999). Parameter-free (meaning without regression) predictions were obtained by Jasper and Miller (2011) and provide a reasonable estimate of low pressure methane decomposition rates. For the unimolecular reaction of methyl isocyanide it was concluded that for reactions at low pressures the collision frequency is the most influential parameter and not the collision efficiency (Matsugi, 2019).

Jasper et al. (Jasper and Miller, 2009) calculated reaction rate constants for different bathing gases over pressure. The rates converge with increasing pressure. This is an extrapolation of the interactions at low pressures towards the high pressure domain. As there are more collisions the reaction rate starts to become less dependent on the molecule itself and the rate determining step becomes the dissociation of the activated molecule (Eq. (2)). This shows that according to current known theories there is no significant effect of the type of bathing gas on the conversion at high pressures.

At low pressure there is a dependency of the reaction rate on the bathing gas (Jasper and Miller, 2011; Matsugi, 2019), but there is no clear trend on the type of bathing gas as was measured in this work in the high pressure domain. The dependency lies mostly in the collision frequency and efficiency.

1.2. Reported experimental observations at high pressure

In literature three studies were found that have possibly measured the same effect (Choudhary et al., 2021; Ezdin et al., 2022; Kolbanovskij et al., 1982). The first authors (Kolbanovskij et al. (1982)) operated a shock tube experimental set-up with a piston, separating the launch gas from the reacting gas. It is similar to the pulsed compression reactor used in this research. They measured N_2O decomposition by compressing it from room temperature and atmospheric pressure up to 250 bar. The results are shown in the left graph of Fig. 3. The deviation in N_2O conversion per noble gas was attributed to cold zones in the gas and it was concluded that xenon has the smallest deviation from adiabatic behaviour.

The second authors (Choudhary et al. (2021)) mention that they observe a difference between their experiments at high pressure (10 bar) of ethanol pyrolysis in argon and the pyrolysis measured by others in neon (Aghsaee et al. (2015) and Kiecherer et al. (2015)). As quoted from their paper: “A possible reason for the observed discrepancy might be the absence of chaperon efficiency for Neon in both models for key pressure-dependent reactions, R1, R2, and R12. The experiments reported by Aghsaee et al. (2015) utilized 1% C_2H_5OH/1% Argon/98% Neon as the test mixture. While plausible, it is unlikely that the identity of the bath gas would have such a significant impact on the rate of evolution of species.”. They rightfully discuss the fact that the findings of Aghsaee et al. and Kiecherer et al. are contradicting each other. However, we would like to point out that the data of Aghsaee et al. shows that the reaction rate is slower in neon compared to argon and that the data of Kiecherer et al. shows the opposite. Irregardless of whether it is faster or slower, the data shows that the reaction rate is not the same as in argon.

Lastly, soot production was investigated in different noble gases including argon, neon and helium by Ezdin et al. (2023, 2022). The focus of the work lies on the characterization of soot, but a lot of compression experiments were performed with maximum pressures ranging from 35 to 100 bar. The authors mention that somehow in helium it is not possible to obtain the same conversion as in neon, during the pyrolysis of investigated precursors for soot (CH_4, C_2H_4 and C_2H_2). The conversion in argon was observed to be higher than in neon. The authors state that the conversion rates scale with the atomic masses or the radii of the atoms. They hypothesise that the small mass of helium and collision cross section significantly limits the kinetics of energy transfer between the bathing gas and reactant, but they do not verify this.

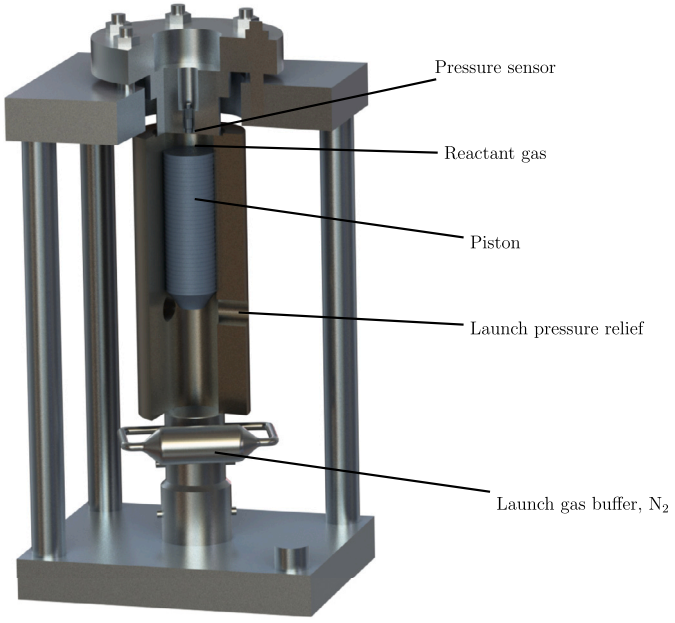

Fig. 1. Overview of the single shot reactor.

The unimolecular reactions of N_2O, CH_4 and CO_2 (called the target molecules) are studied in the bathing gases helium, neon, argon, xenon and H_2 at high pressures to understand the effect of the bathing gas on the reaction rate. First the experimental results of N_2O decomposition and CH_4 pyrolysis are presented. Then the experimental results of CO_2 are shown and analysed with a kinetic model. After that, a possible theory is proposed that could explain the observed behaviour.

2. Experimental methods and data analysis

To understand reactions at high pressures experiments have been done with 4%$_{mol}$ N_2O, 2%$_{mol}$ of CO_2 and 1%$_{mol}$ of CH_4 diluted in an inert gas. All percentages in this paper are in mol. 4% of N_2O was used to replicate the experiments of Kolbanovskij et al. (1982). 2% CO_2 is used to make sure that sufficient amounts of products could be measured due to the expected low conversion. The high dilutions are used to approach an adiabatic curve and make temperature changes caused by reactions as small as possible. The experiments are performed with noble single atomic gases to mitigate any non-ideal behaviour and stay as close to ideal gases as possible. As a last benefit, these single atomic molecules have the lowest heat capacity, meaning that temperatures up to 4000 K can be reached in the PCR, which is expanding the experimental domain. For methane pyrolysis experiments, hydrogen is used as a diluent to obtain a reference point.

The schematic representation of the research reactor called the Single Shot Reactor (SSR) is shown Fig. 1. The working principle of the reactor is to use a precisely machined core cylinder (Corrax) and piston (graphite). The gap between piston and wall lies between 10 and 20 μm and acts as a sealing. Due to thermal expansion differences there is a piston for each reactor temperature. More details about the experimental set-up, the procedure and the calculation of conversion and selectivity for the methane system can be found in a previous publication (Slot-

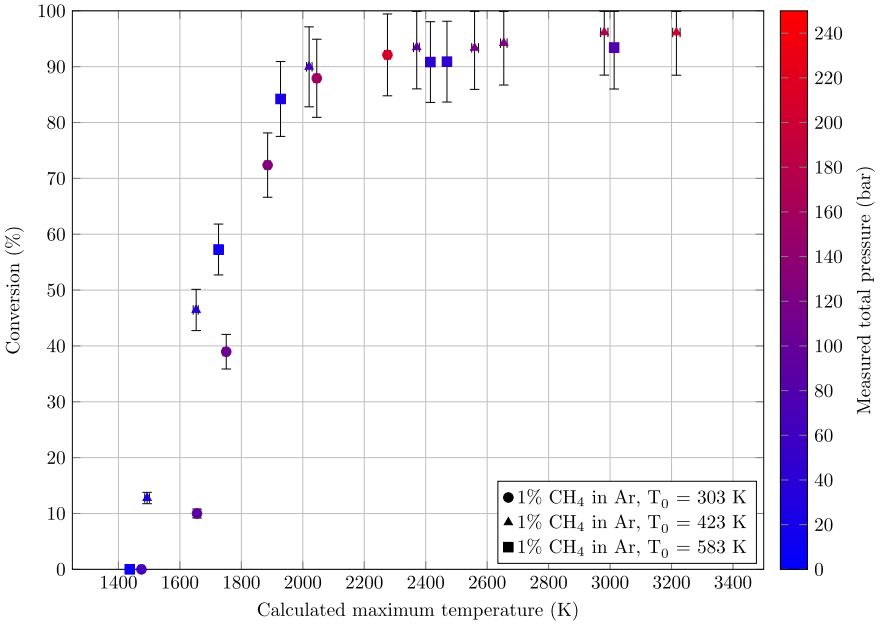

Fig. 2. Conversion of methane in argon for different initial gas temperatures plotted over the maximum calculated temperature (K). The colour bar indicates the measured pressure.

boom and Kersten, 2023). The calculation of the conversion of N_2O and CO_2 is explained in the Supporting Information.

Experiments were done at three different initial gas and reactor temperatures of 303 K, 423 K and 583 K. There are two methods of performing experiments. The first is to create a single pulse by one launch, the amount of launch gas released is just enough to create a single pulse and all the subsequent ones are negligible. The second is done by releasing more gas into the chamber to get multiple pulses in one launch, the pressure is measured of all pulses. In both cases the initial temperature of the gas is equal to the reactor temperature and a sample is taken after the pulse(s). The pressure pulse is accurately measured in the top chamber by the Optrand AutoPSI-TC Sensor model DB2287, rated from 0-1000 bar. The calibration curve is shown in the Supporting Information of a previous paper (Slotboom and Kersten, 2023). The compression ratio is measured by the displacement of a metal pin by the piston.

The maximum measured pressure and feed composition is used to interpret the data and calculate the temperature. The maximum measured pressure is fed to a reactor model, where the pressure of the launch gas in a virtual buffer is changed to match the measured pulse. After that, this launch pressure set-point is an input to the model that also includes reactions. At all times, an equation of state is used to describe the pressure, temperature and volume during a compression. The GERG-2008 equation of state in the form of the Helmholtz free energy is used (Kunz and Wagner, 2012; Span and Wagner, 2003), with the addition of N_2O from another paper (Lemmon and Span, 2006). The used reactor and compression model is explained in detail in a previous publication (Slotboom and Kersten, 2023).

3. Experimental results

Over 100 single shot experiments with three different reactions in four noble bathing gases are measured in one reactor, of which one reaction shows the same trend measured by Kolbanovskij et al. in a different reactor (Kolbanovskij et al., 1982).

The influence of the type of bathing gas was first encountered in methane pyrolysis experiments, but in methane pyrolysis the subsequent reaction network is too complex to interpret. N_2O was tested to check if the same trend as Kolbanovskij et al. could be measured. CO_2 was introduced as a third reaction for measuring the dependence on the inert bathing gas.

3.1. Results of methane pyrolysis in argon

Experiments were done with 1% CH_4 in argon where the initial temperature of the gas was 303, 423 and 588 K, the results are shown in Fig. 2. The launch pressure was varied between 10 and 120 bar to reach similar conversion levels. This provides a comparison of conversion at similar temperatures, but different pressures and concentrations. Methane was chosen because the reaction temperatures can be reached from all three initial gas temperatures.

Compressing a gas from a higher initial temperature means that the same maximum compression temperature is reached at lower pressures. Around 2500 K the concentrations are 950, 430 and 200 mol m^{-3} for initial temperatures of respectively 303, 423 and 588 K. Despite such differences in concentration, the conversion is the same in all cases, this is shown in Fig. 2. This set of experiments confirms that the PCR operates in the high pressure domain, where the conversion rate is independent of the total concentration of the bathing gas ([I]). The pressure is a factor 4 and concentration almost 5 higher at the same temperature when going from 583 K to 303 K initial gas temperature, but the conversion remains the same.

3.2. Results of N_2O decomposition

N_2O decomposition is a reaction with only nitrogen and oxygen as a product. The initial step is shown in Eq. (4). Kolbanovskij et al. (1982) chose to investigate this reaction to measure any deviation from adiabaticity. They deemed N_2O decomposition the best candidate, because it does not suffer from equilibrium limitations ($K_{c,298K} = 5.3 \cdot 10^{16}$ $\sqrt{\text{mol/m}^3}$).

$$N_2O \leftrightarrows N_2 + \frac{1}{2}O_2 \quad (\Delta_r H_{298K} = -81.6\ \text{kJ/mol}) \tag{4}$$

In Fig. 3 the conversion is plotted over the compression ratio. One should realize that at the same compression ratio the temperature and pressure are identical for all bathing gasses. High conversion levels of N_2O are quickly reached in xenon as shown in Fig. 3 by the data of Kolbanovskij et al. (1982). The conversion in argon is much lower than in

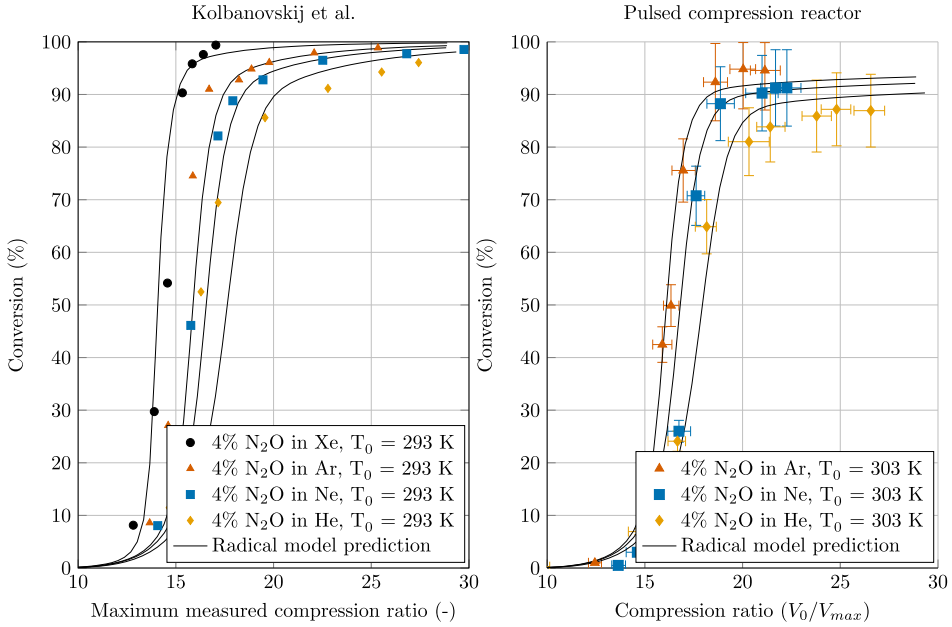

Fig. 3. On the left: Conversion of 4% nitrogen oxide diluted in inert noble gases plotted over the measured compression ratio, reproduced from Kolbanovskij et al. (1982). On the right: Decomposition of 4% nitrous oxide measured in the PCR in the bathing gases argon, neon and helium. Experiments are a duplicate of the experiments done by Kolbanovskij et al. (1982). The trend of the bathing gas dependency on the conversion is the same. At the compression ratio of 27 the measured pressure was 200 bar and the calculated temperature is 2050 K.

xenon dilutions at low compression ratios (<17). And N_2O decomposition rates are even slower in neon and helium dilutions.

The experiments in the PCR were done with an initial gas and reactor temperature of 303 K and the maximum measured pressure over all experiments was 200 bar with a calculated temperature of 2050 K. In the PCR the same effect and trend was measured for argon, neon and helium. However, the conversion in the PCR does not go towards 100%, while this is the case for the data of Kolbanovskij et al. The difference could originate from the fact that the measurements of Kolbanovskij et al. were done in a device with a longer stroke and a bronze piston that is five times as heavy. Another difference is that they were able to perform a perfect quench with a special mechanism. After the piston was set in motion, the remaining launch gas was completely evacuated from below the piston. This creates a rapid and perfect quench. In the PCR the expansion curve is nearly identical to the compression curve, because the piston still compresses the remaining launch gas below the piston during the return phase. However, a large enough portion of the launch gas is still released to prevent any subsequent pulses. The model predictions shown in Fig. 3 are produced by a kinetic model that includes radical species and is regressed only on the data of the PCR, this is shown later.

Kolbanovskij et al. attributed the observed difference in N_2O decomposition rates to cold zones in the gas (i.e. temperature differences and deviation from adiabatic compression). When only the N_2O reaction is investigated this can be a possible explanation. For example, helium has the highest thermal conductivity. However, when looking at the later presented CO_2 data, which show an opposite trend, this cannot be the case.

3.3. Results of methane pyrolysis in different bathing gases

Methane dissociates into a methyl and a hydrogen radical in the first activation step as shown in Eq. (5), after which many products form. All these reactions are endothermic. The reaction network is complex and especially the role of the hydrogen radical in the context of the observed dependency on the type of bathing gas is unclear. However, irregardless of this, measurements can still prove the existence of it.

$$CH_4 \leftrightarrows CH_3\cdot + H\cdot \quad (\Delta_r H_{298K} = 438\ \text{kJ/mol}) \tag{5}$$

Initial experiments were done with 1% of CH_4 diluted in xenon, argon and helium. The mixtures were compressed from an initial gas temperature of 583 K (and atmospheric pressure) up to 150 bar and up to a calculated 3800 K. All the points lie within the error margin. Therefore, these results are shown in the Supporting Information. To increase the difference in conversion 5% H_2 was added in order to lower the conversion rate (Slotboom and Kersten, 2023).

The conversion of methane with hydrogen plotted over the calculated maximum temperature is shown in Fig. 4. The gap in conversion between the inert gases is large enough that the data falls outside of the measurement error. The difference in conversion between helium and xenon varies between 20 to 25%. The trend of methane conversion is the same as was observed for N_2O decomposition. The heavier the gas the higher the conversion, while the temperature is the same.

From 2000 K to 3800 K the methane conversion goes towards a constant value for each noble gas. The conversion in helium never reaches the same levels as argon and xenon over a 2000 K temperature difference. This is one of the strongest indicators that the type of bathing gas influences the decomposition of methane at the investigated conditions in the PCR.

A 2000 K difference is significant enough to rule out any cold zone effects as suggested by Kolbanovskij et al. (1982). If there is any temperature drop effect, the exponential increase in reaction rate should bring conversion levels in helium to the same values as neon, argon and xenon in this domain. An analysis of temperature drop due to leakages is shown in the Supporting Information. It is concluded that this cannot be a cause either. The later shown CO_2 data is also an indication that it cannot be a leakage effect. Following the discussion above, there is only one difference left between the four bathing gases, which is the nature of the molecules themselves.

Fig. 5 shows methane pyrolysis results from 1600 to 3200 K in a mixture with 1% CH_4 and a ratio of 1:50 of CH_4 to H_2. The influence of the type of bathing gas seems to have disappeared, because no matter which noble gas is used for filling the remainder of the gas, all experimental data points are on one line. The experiments with pure hydrogen

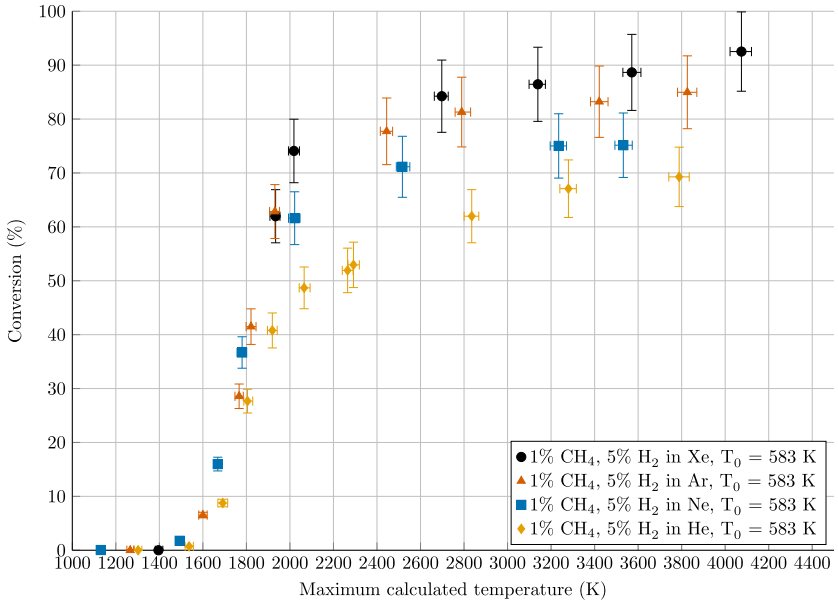

Fig. 4. Conversion of 1% CH_4 plus 5% H_2 diluted in different noble gases and hydrogen plotted over the calculated maximum temperature.

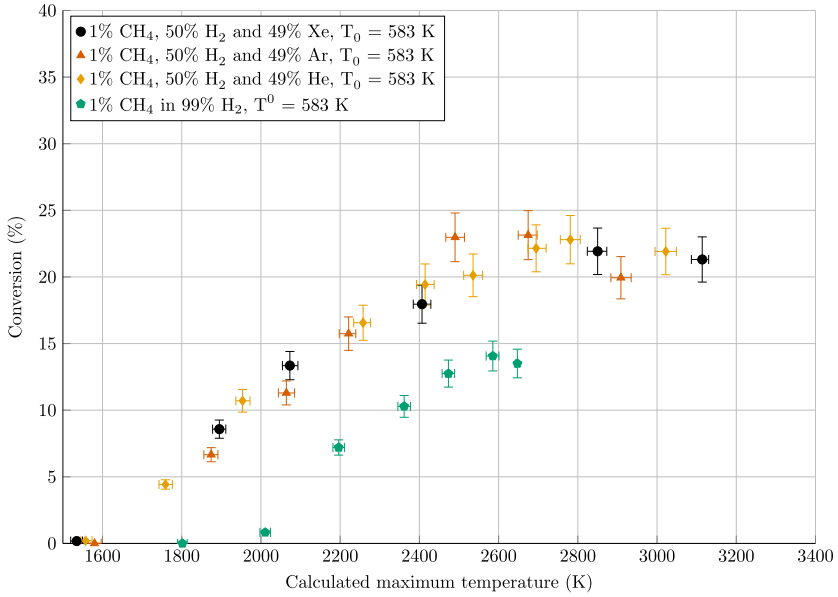

Fig. 5. Conversion of 1% CH_4 plus 50% H_2 diluted in different noble gases and hydrogen plotted over the calculated maximum temperature.

as bathing gas are showing the minimum boundary of methane conversion.

The temperature at which conversion is measured in the 50% H_2 experiments begins between 1800 and 2000 K. The observed conversion is determined by the reverse reaction and interaction with the hydrogen. Without a sophisticated kinetic model it is not possible to draw any more conclusions from this data. However, the fact that there is a mixture available that measures no difference for types of bathing gases is additional proof that it is not a device or measurement specific effect. If it would be a device specific effect there would be an influence of the type of bathing gas under all conditions.

3.4. Results of CO_2 dissociation

This section discusses the measured dependency of the type of bathing gas on the dissociation of CO_2. The results are shown in Eq. (6). First the experimental results are presented and then a simplified kinetic model is introduced, which is used to analyse the concentration profiles during a pulse.

$$CO_2 \leftrightarrows CO + \frac{1}{2}O_2 \quad (\Delta_r H_{298K} = 283 \text{ kJ/mol}) \tag{6}$$

Fig. 6 shows the conversion of CO_2 diluted in argon, neon, helium and a mixture of helium and neon plotted over the calculated temperature. The data series where 37% of helium was added to neon was done to get an extra data-point that matches an average molar mass of 15 $g\,mol^{-1}$.

The conversion is much lower in neon and argon than in helium. This is the reverse of the observed trend of the N_2O and CH_4 reactions. The reverse trend seems unexpected. A kinetic model is introduced in the section below as an attempt to explain this. There is a gap in conversion between argon and helium, the maximum measured conversion of CO_2 in a single shot for argon is 8%, while a dilution with helium gives almost a factor two higher. The CO_2 conversion of the neon/helium mixture lies in between helium and neon, leaning more towards

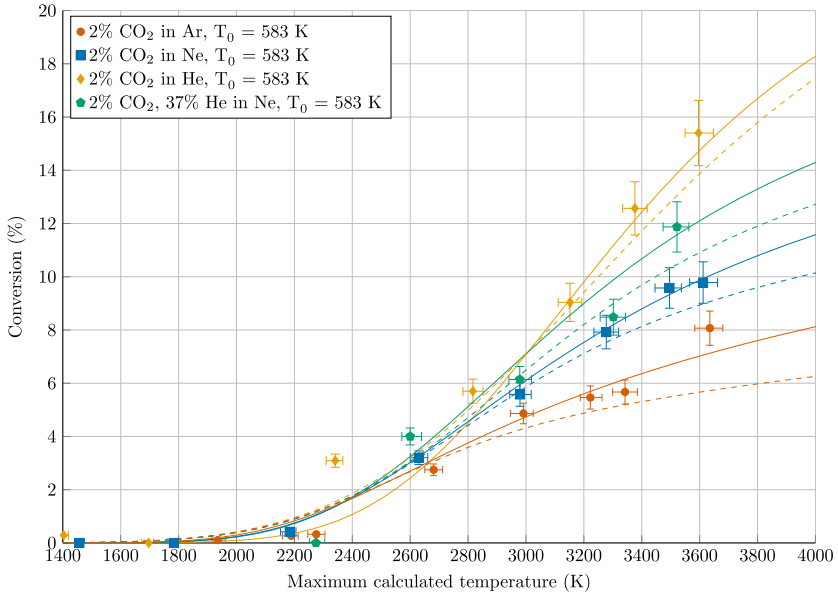

Fig. 6. CO_2 conversion plotted over the maximum calculated temperature. The conversion is based on the CO_2 measurement. The dashed lines are KME predictions according to Eqs. (8) and (14) to (16) with the parameters as shown in Table 2. The dashed lines are the radical model predictions.

neon. Unfortunately, the error in this data is too large to draw any conclusions. Mixtures of noble gases are something to be investigated further.

3.4.1. Simplified kinetic model and regression

The pulsed compression reactor has a complex trajectory of changing volume, pressure and temperature all at the same time. A reactor model has been previously developed and verified that is suitable for implementing kinetics as well (Slotboom and Kersten, 2023).

$$CO_2 \leftrightarrows CO + \frac{1}{2}O_2 \tag{7}$$

The choice has been made to only describe the overall molecular reaction (Eq. (7)), resulting in the rate equation as shown in Eq. (8). Later a radical model is introduced that is regressed on the CO_2 and N_2O data simultaneously.

$$R_{CO_2} = k^+[CO_2]\left(1 - \frac{1}{K_c(T)}\frac{[CO][O]^{\frac{1}{2}}}{[CO_2]}\right) \tag{8}$$

The forward reaction rate is regressed while using the equilibrium constant for calculating the reverse reaction rate, as shown in Eq. (8). This is a total of 2 parameters per bathing gas. The relationship for $K_c(T)$ is a polynomial derived from the Gibbs free energies of the components and is given in the Supporting Information.

$$k^+ = k_0^+ exp\left(\frac{-E_A^+}{RT}\right) = exp\left(A + B\left(\frac{T - T_{ref}}{T}\right)\right) \tag{9}$$

All parameters are regressed in the re-parametrized form of the Arrhenius equation to reduce cross-correlation of the activation energy and the pre-exponential factor (Schwaab et al., 2008), as given in Eq. (9). Only the original Arrhenius parameters are given in Table 1.

$$MSE = \frac{1}{N_{exp}}\left(y_{CO_2,out} - \hat{y}_{CO_2,out}\right)^2 \tag{10}$$

A least square fit is performed with the mean square error as the objective function as defined in Eq. (10). N_{exp} is the number of experiments.

Table 1 gives the results of the regression. After a first regression of both k_0^+ and E_A^+ it turned out that between the bathing gases the activation energy hardly changes (range was between 271 and 283 kJ/mol),

Table 1
Regressed parameters for CO_2 dissociation per noble gas for the forward reaction rate, with the K_{EQ} for the reverse rate. The activation energy has been averaged from initial fits and set as a constant to be able to compare the k^+.

	k_0^+ [s^{-1}]	E_A^+ [kJ mol^{-1}]	MSE_i
Argon	$5.82 \cdot 10^7$	277	$2.8 \cdot 10^{-5}$
Neon	$4.19 \cdot 10^7$	277	$3.1 \cdot 10^{-6}$
Helium	$2.46 \cdot 10^7$	277	$9.9 \cdot 10^{-5}$

but the pre-exponential factor does. In the further regression procedure the average of 277 kJ/mol was used. This may be rationalized by the fact that the activation energy is an intrinsic reaction property of the activated molecule (CO_2) itself. It is considered to be independent of the bathing gas.

The resulting pre-exponential factors for argon, neon and helium with equal activation energies are plotted over the molar mass of the inert gas in Fig. 7. Fig. 7 shows that the reaction rate is dependent on the molar mass. The correlation is: the heavier the bathing gas, the faster the reaction. This regressed dependency is following the same trend as the data of N_2O decomposition and CH_4 pyrolysis.

$$k_0^+ = k_{zero} + C\beta \tag{11}$$

$$\beta = \frac{M_{w,I}}{M_{w,M}} \tag{12}$$

Fig. 7 shows two options for describing the relation of k_0^+ with regard to the molar mass. The first is to introduce a linear relationship between k_0^+ and β as given in Eq. (11). β is defined in Eq. (12).

$$k_0^+ = k_{zero} exp\left(C\sqrt{\beta}\right) \tag{13}$$

The second option is to introduce a linear relationship between the logarithm of k_0^+ and the square root of β, as shown in Eq. (13). The square root is introduced to get the best fit of the data points.

Fig. 7 shows that this version of describing the relation of k_0^+ is just as good as the linear one. The benefit of using the exponential version is that it satisfies the chemical equilibrium. This is because the term $exp\left(C\sqrt{\beta}\right)$ is present both in the forward and backward reaction rate

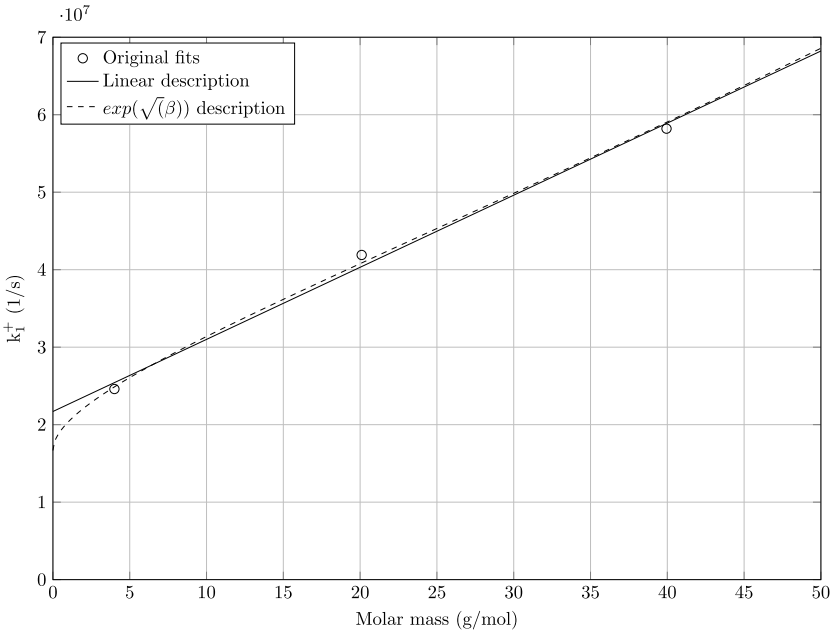

Fig. 7. Ways of displaying the experimentally obtained relationship between the k_0^+ and the molar mass of the inert bathing gas.

and cancels out at equilibrium. For this reason the exponential form is chosen.

It is our hypothesis that the exponent represents the equilibrium of activation of a species versus deactivation $\left(\frac{k_1}{k_{-1}}\right)$, this is the equilibrium of the reaction as shown in Eq. (1).

When the average molar mass of the mixture is used to calculate β the prediction of the helium/neon mixture is far off. Based on the experimental data, the average molar mass cannot be used. A mixture dependent k_0^+ is introduced for calculating mixture rate properties, as shown in Eqs. (14) to (16). This mathematical description means that the total reaction rate in a mixture is equal to the sum of individual reaction rates in one type of bathing gas, multiplied by the mole fraction. In other words, collisions occur between molecules and not between a reactant and an 'average' bathing gas molecule.

k_0^+ of Eq. (8) is now replaced with the one as given in Eq. (14).

$$k_0^+ = f_{mix} k_{zero} \tag{14}$$

k_{zero} is the reaction rate of the species (CO_2) decomposition in absolute vacuum, without any collision. f_{mix} is given in Eq. (15) and it is the factor that is dependent on the molar mass of the bathing gas.

$$f_{mix} = \sum_j^{N_c} y_j exp\left(C_\beta \sqrt{\beta_j}\right) \tag{15}$$

β_j is defined in Eq. (16) and C_β is the correction factor for the, at this point unknown, dependency of the species on the bathing gas. When β is one (and also $y_{CO_2} = 1$), the factor f_{mix} adjusts k_{zero} to the reaction rate when colliding with itself only (i.e. the pure gas). Any other β is for (a mixture of) other bathing gases.

$$\beta_j = \frac{M_{w,j}}{M_{w,CO_2}} \tag{16}$$

From the individual regression parameters as shown in Table 1, the mixture parameters are calculated and shown in Table 2. The resulting prediction of CO_2 conversion with these parameters is shown in Fig. 6.

The results above show: the heavier the bathing gas, the faster the reaction. This section below describes how is it possible that this is the outcome when the observed trend in Fig. 6 shows the opposite. All the predictions are done with the parameters as shown in Table 2.

Table 2
Calculated mixture parameters for describing the effect of the type of bathing gas on the CO_2 decomposition at high pressures. The resulting prediction is shown in Fig. 6.

k_{zero} [s^{-1}]	E_A^+ [kJ mol^{-1}]	C_β [-]	$MSE_{\text{all data}}$
$1.667 \cdot 10^7$	277.47	1.3269	$4.95 \cdot 10^{-5}$

Multiple shots were performed with 2% CO_2 in argon to check whether or not a higher conversion could be obtained. The results and internal profiles predicted by the kinetic model are shown in Figs. 8 and 9. Increasing the amount of shots effectively increases the residence time. The measured pressure profile is shown in the Supporting Information.

Fig. 8 shows the conversion and temperature during the first of the four pulses, including the experimental result after one pulse. Initially the conversion of CO_2 in argon is higher, because the reaction rate in heavier gases is higher. However, also the reverse reaction is faster. In the expansion phase of the pulse with argon as diluent, most of the produced carbon monoxide reacts back to CO_2. In helium this occurs at a slower rate, giving an apparent higher conversion of CO_2.

Fig. 9 shows the four pulses, they all reach sufficiently high temperatures of between 2800 K and 3200 K. The measured CO_2 conversion when diluted in argon was still only 9%, 1% higher than in a single shot. Slowly the conversion goes up, but in argon it seems not possible to reach similar levels of conversion as in helium. With each pulse the expansion side has the most influence on the final observed conversion. The amount of pulses has a minimal effect on the CO_2 conversion in argon, because each time during the quench most of the CO reacts back faster than in helium.

Fig. 10 shows the extent of the effect under different circumstances. The decomposition of CO_2 is plotted over time in a hypothetical closed box set-up at a constant temperature of 3000 K. It shows that the reaction rate is much higher in argon, but both bathing gases still reach equilibrium in around 10 ms. This is also a requirement, because the

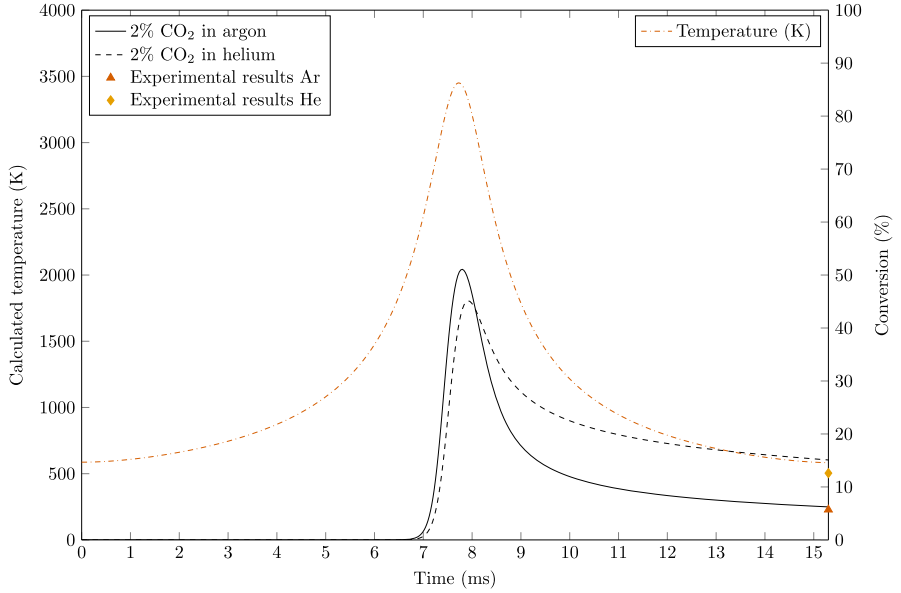

Fig. 8. Simulation of the first pulse of the unimolecular reaction of 2.1% CO_2 in helium and argon plotted over time. The temperature profile is shown on the right y-axis. This temperature is the same for both helium and argon.

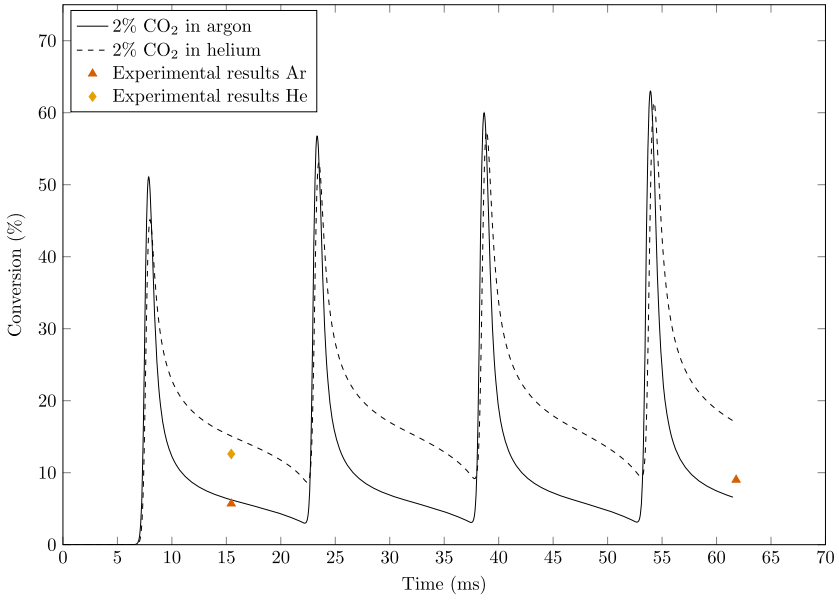

Fig. 9. Simulation of the unimolecular reaction of 2.1% CO_2 in helium and argon plotted over time. This is a simulation of the experimental result of four pulses with Method 2, the measured pressure profile is shown in the Supporting Information. The first pulse is the same as Fig. 8.

bathing gas cannot and should not affect the molecular equilibrium conversion.

3.5. Combined radical model for CO_2 and N_2O

Molecular oxygen and oxygen radicals are both present in the CO_2 and the N_2O decomposition reactions. Therefore, both systems can be described with a common reaction rate for the oxygen splitting and recombination as shown in Eq. (17). CO_2 decomposition is endothermic and performed in a different domain than the exothermic N_2O decomposition. Predicting both in a single kinetic system can provide more information. This is useful for regressing the additional parameters when working with radicals.

$$O_2 \leftrightarrows O\cdot + O\cdot \tag{17}$$

The remaining radical reactions for CO_2 and N_2O are shown along the regressed parameters in Table 3. The reaction equations with a β above the arrow mean that this part of the reaction is dependent on the mass of the bathing gas. Hence, one molecule on that side of the reaction has to be activated. It must be noted that this is a regression attempt, but there is no certainty that the global minimum was reached. Many attempts were made to regress the system with other configurations of mass dependent reactions (for example on all sides of the reaction equations), but the presented set in Table 3 was the only found set of parameters that could predict both CO_2 and N_2O experiments well. This does not mean that other combinations are not possible. The aim here is to prove that a set of parameters exists that can predict all experiments. This is done to show that the observed dependency on the type of bathing gas is indeed a plausible kinetic effect.

It cannot be ruled out that this effect solely belongs to unimolecular reactions. The reverse reaction of the CO_2 decomposition can be con-

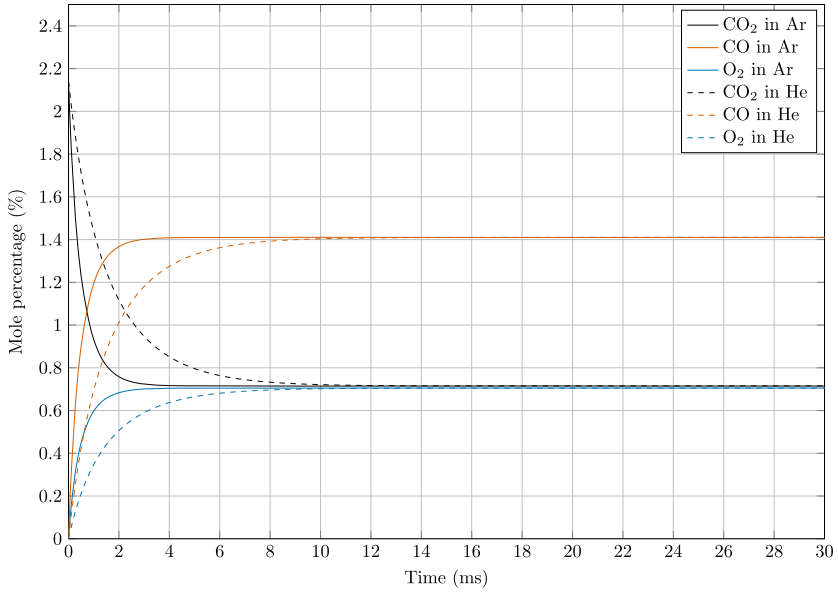

Fig. 10. Simulation of the unimolecular reaction of 2.1% CO_2 in helium and argon plotted over time. The model used is given in Table 2. This is a closed box with no volume change and a temperature of 3000 K.

Table 3
Radical model overview and regression results of the bathing gas type dependent parameter C_β.

	C_β
$CO_2 \overset{\beta}{\rightleftarrows} CO + O\cdot$	0
$CO + O_2 \overset{\beta}{\rightleftarrows} CO_2 + O\cdot$	2.64
$O_2 \overset{\beta}{\rightleftarrows} O\cdot + O\cdot$	2.64
$N_2O \overset{\beta}{\rightleftarrows} N_2 + O\cdot$	0.205
$N_2 + O_2 \overset{\beta}{\rightleftarrows} N_2O + O\cdot$	0

sidered to go via a two step reaction pathway for example, as shown in Eqs. (18) and (19). This is mathematically not distinguishable from a single unimolecular reaction (like in Eq. (4)) in the high pressure domain, where the reaction of an activated species is rate determining.

$$CO + I \rightleftarrows CO^* + I \tag{18}$$

$$CO^* + O_2 \rightleftarrows CO_2 + O\cdot \tag{19}$$

The beta of the first decomposition reaction of CO_2 in Table 3 can be zero, because the net conversion is fully determined by the reverse reaction. What happens during compression and at the peak of the pulse does not matter. Actual experimental information about CO or CO_2 percentages during (or at maximum conditions in the peak of) the pulse is not available.

The resulting predictions for N_2O are plotted in Fig. 3. CO_2 results are shown in Fig. 6 with dashed lines. The regression was only performed on the data of the PCR. The radical model that uses the $exp\left(C_\beta\sqrt{\beta}\right)$ term is well able to predict the data of Kolbanovskij et al., as shown in Fig. 3. This is a remarkable result, as xenon was never part of neither the CO_2 or N_2O dataset in the PCR.

4. Proposed explanation for the presence of beta in the rate equation

This section provides a description of a possible theory that could explain why the experimental results depend on the bathing gas at high pressures. This is not a final theory, but it is one that makes a first attempt at understanding the relation between the observed reaction rate and the molar mass of the bathing gas.

At a molecular level molecules collide with each other. In those collisions energy is transferred from one molecule to the other. At high temperatures and pressures millions of collisions take place per second. The amount of collisions is strongly dependent on the pressure. When you increase the pressure from atmospheric to 100 bar the amount of collisions will also increase by a factor 100.

The amount of energy that is transferred in a single collision can be calculated by solving energy and momentum balances for an elastic collision, as shown in Eqs. (20) and (21). In which $M_{w,I}$ is the molar mass of the inert gas (or bathing gas) and $M_{w,M}$ is the molar mass of the target molecule that can undergo a unimolecular reaction. v_i^1 are the initial molecular velocities and v_i^2 are the velocities after the collision.

$$\frac{1}{2}M_{w,I}(v_I^1)^2 + \frac{1}{2}M_{w,M}(v_M^1)^2 = \frac{1}{2}M_{w,I}(v_I^2)^2 + \frac{1}{2}M_{w,M}(v_M^2)^2 \tag{20}$$

$$M_{w,I}v_I^1 + M_{w,M}v_M^1 = M_{w,I}v_I^2 + M_{w,M}v_M^2 \tag{21}$$

After solving the set of equations (Eqs. (20) and (21)), there are two resulting equations. They give the velocity of the two colliding molecules after the collision, as shown in Eqs. (22) and (23).

$$v_M^2 = \frac{M_{w,M} - M_{w,I}}{M_{w,M} + M_{w,I}}v_M^1 + \frac{2M_{w,I}}{M_{w,M} + M_{w,I}}v_I^1 \tag{22}$$

$$v_I^2 = \frac{2M_{w,M}}{M_{w,M} + M_{w,I}}v_M^1 + \frac{M_{w,I} - M_{w,M}}{M_{w,M} + M_{w,I}}v_I^1 \tag{23}$$

Which can be rewritten into Eqs. (24) and (25).

$$\frac{v_M^2}{v_M^1} = \frac{1-\beta}{1+\beta} + \frac{2\beta}{1+\beta}\frac{v_I^1}{v_M^1} \tag{24}$$

$$\frac{v_I^2}{v_I^1} = \frac{\beta-1}{1+\beta} + \frac{2}{1+\beta}\frac{v_M^1}{v_I^1} \tag{25}$$

With β defined as in Eq. (12).

A situation is considered where a target molecule (M), for example N_2O, is not activated nor deactivated by a collision with a bathing gas molecule. This means that it loses no energy through a collision. It is assumed that the kinetic energy of M is equal to the average kinetic energy $\left(\frac{3}{2}RT\right)$, from which the initial velocity of the molecule can be

Table 4
Calculations of full frontal collisions between an average N_2O molecule and an inert gas, calculations are independent of pressure, the temperature is 2000 K and pressure where applicable 100 bar. All collisions are calculated in such a way that they will not deactivate the N_2O. The kinetic energy after the collision is still $\frac{3}{2}RT$, $v_M^1 = 1065$ m/s.

	Xenon	Argon	Neon	Helium
v_I^1 [m s^{-1}]	-360	-1200	-2300	-12000
E_I^1 [kJ mol^{-1}]	8.4	27	55	270
Percentage of molecules $>= v_I^1$ [%]	80	34	8.5	$3.2 \cdot 10^{-5}$
Collisions [$\cdot 10^{11}$ s^{-1}]	1.6	2.1	1.9	3.8

calculated (Eq. (26)). In a diluted situation the chances are the highest it will collide with the bathing gas (or inert gas I). The collision is assumed to be frontal. The direction of the initial inert gas velocity is negative.

It can be calculated how fast the bathing gas molecule needs to be, in order to not activate nor deactivate the target molecule. The previously derived relations in Eq. (12) can be used and rearranged to obtain one expression for the initial velocity of the inert molecule (I), as shown in Eq. (28). Once the velocity is known, the energy of this single molecule can also be calculated (Eq. (29)).

$$v_M^1 = -\sqrt{\frac{2E_M^1}{M_{w,M}}} \tag{26}$$

$$v_I^1 = v_M^1 \frac{1+\beta}{2\beta}\left(-\sqrt{\frac{E_M^2}{E_M^1}} - \frac{1-\beta}{1+\beta}\right) \tag{27}$$

$$v_I^1 = v_M^1 \frac{1+\beta}{2\beta}\left(-1 - \frac{1-\beta}{1+\beta}\right) = -v_M^1 \frac{1}{\beta} \tag{28}$$

$$E_I^1 = \frac{1}{2} M_{w,I} \left(v_I^1\right)^2 \tag{29}$$

Eq. (28) is a trivial solution to the problem and the solution is the conservation of momentum itself. Therefore, the initial velocity of the inert in this scenario is linearly dependent on its mass and the mass of the other molecule M. When βv_I^1 is higher than the initial velocity of M, then M will gain in energy. The energy that the inert gas needs in order to keep the other molecule (M) at the same velocity (and energy) as before the collision is given in Eq. (30). This relation states that a heavier molecule needs less energy to do that. The calculation results for several inert gases are shown in Table 4.

$$E_I^1 = \frac{1}{2} M_{w,I}\left(-\sqrt{\frac{2E_M^1}{M_{w,M}}}\frac{1}{\beta}\right)^2 = E_M^1 \frac{1}{\beta} = E_M^1 \frac{M_{w,M}}{M_{w,I}} \tag{30}$$

Eq. (30) represents the initial energy needed of the inert gas to keep M at the same energy level. From the perspective of the target molecule M the energy it maintains in collisions is proportional to the energy of the inert times β, as shown in Eq. (31).

$$\frac{E_M^1}{E_I^1} = \frac{M_{w,I}}{M_{w,M}} = \beta = \frac{\frac{1}{2} M_{w,M} v_{M,1}^2}{\frac{1}{2} M_{w,I} v_{I,1}^2} \tag{31}$$

The percentage of the bathing gas molecules that have sufficient energy to not slow down the reactant molecule (i.e. able to give N_2O a higher translational energy) can be calculated. This is done by integrating the Maxwell-Boltzmann distribution of molecular velocity from the calculated v_I^1 to infinity. This fraction is different for each type of bathing gas, as shown in Table 4.

Table 4 shows that when energy is transferred through an elastic collision, high velocities are needed for helium. Since xenon has such a large mass, it needs much lower velocities (and energy per molecule) to be able to keep the target molecule at the same energy level. The heavier gases contain a much larger percentage of molecules that are able to activate N_2O.

The bathing gas (or the most dominant species) is ultimately the one that is most apparent in transferring energy through collisions. This means that a (unimolecular) decomposition at high pressures in light bathing gases is slower, because there is only a tiny fraction of molecules available. Only those have large enough velocities to be able to transfer energy to the target molecule (M). Deliberately the term slower is used, because there ís a fraction of molecules with sufficient kinetic energy. When kept at the same temperature for an infinite amount of time it can still reach similar conversions and thus thermodynamic equilibrium.

There are more collisions per second in helium, because the velocity is higher. But the higher amount of collisions per second in helium is not going to cancel out the effect of the energy transfer in a single collision.

The activation energy of the target molecule remains the same, since it is a (unimolecular) decomposition independent of any other species. The internal decomposition is the rate limiting step, it is the time it takes to dissociate once it reaches the activation energy. This is independent of the bathing gas and could be imagined to take place in the empty space in between collisions.

To summarize, the reaction rate of a (unimolecular) reaction is dependent on the product of the fraction of molecules with sufficient energy to react (the well-known Arrhenius equation) and the ability of the bathing gas to provide this. This ability is reflected by the inverse of the amount of energy a single bathing gas molecule needs in order to keep the activated molecule active. The more energy is needed for this, the slower the overall reaction rate in this mixture.

The proposed explanation is one possibility. Other explanations were not explored, because the proposed one was deemed most probable. Differences other than the molar mass exist. For example, variations could arise in chemical properties like polarizability, ionization energies and van der Waals interactions. The first two are unlikely, because there is no electric field and pressures are high. And Van der Waals interactions are expected to be negligible at the calculated temperatures. However, additional (theoretical) work is needed to substantiated these explanations.

5. Conclusion

The decomposition reactions of N_2O, CH_4 and CO_2 were studied in the pulsed compression reactor under high pressure conditions in different inert bathing gases (Xe, Ar, Ne and He). The diluted species were compressed to different conditions ranging up to a maximum pressure of 250 bar and temperature of 4000 K. It was experimentally confirmed with methane pyrolysis experiments that the PCR operates in the high pressure regime.

The experiments with N_2O were a replica of measurements as previously done in a different compression device by Kolbanovskij et al. (1982). Both the data of Kolvanovskij et al. and the data measured in the PCR show that the N_2O decomposition rate is the highest in the most heavy noble gas, and goes down as the molar mass of the bathing gas decreases. Pyrolysis of 1% CH_4 plus 5% H_2 in the PCR showed a similar trend where dilutions in heavier gases reached the highest conversion. The maximum measured difference in CH_4 conversion at similar conditions between helium and xenon is 25%.

The measurements of CO_2 decomposition showed an opposite trend. The highest measured conversion of CO_2 was 15% after a single pulse when diluted in helium, which is more than when using neon. The observed conversion in argon is lower than in neon. A kinetic analysis showed that the data is best described with reaction rates that are higher in heavier gases. The explanation of the reverse trend is that even though the reaction rate is higher in heavier gases, the CO oxidation reverse reaction that takes place in the expansion phase of the pulse is the dominant factor in the net observed conversion. A slower reaction rate in lighter gases stops the reverse reaction sooner.

It was found that the best description of the data is obtained with a factor $exp\left(C\sqrt{\frac{M_{w,I}}{M_{w,M}}}\right)$ in front of the pre-exponential factor of the Arrhenius equation for both the forward and backward reaction. This means that the pre-exponential factor now scales with the molar mass of the bathing gas. C is the dependency on the bathing gas (I) of the specified decomposition rate of molecule (M). It was shown, by energy and momentum balances in combination with the Maxwell-Boltzmann distribution, that for heavier inert gas molecules a larger fraction contains enough energy to activate a reacting molecule.

6. Implications

The measured dependency on the type of bathing gas can provide more data about a reaction when measured in different bathing gases. This can result in more precise estimations of the frequency factor and activation energies. It could potentially give more insight into the underlying radical reactions, including determining whether or not it is a unimolecular reaction. Any application of this effect is so far limited, but one could think of using heavier gases to increase the rate of reaction in short high pressure processes, like combustion or potentially even in a nuclear fusion process.

Declaration of competing interest

The authors declare that they have no known competing financial interests or personal relationships that could have appeared to influence the work reported in this paper.

Data availability

Data will be made available on request.

Acknowledgements

The authors thank Aayan Banerjee for his initial thoughts and help on the observed experimental differences. Many thanks to the technicians of the High Pressure Lab: Benno Knaken for all his efforts to make this reactor operate as best as possible and with high precision, Johan Agterhorst for ordering, changing and connecting countless gas bottles and Ronald Borst for asking questions and thinking along. We thank the project partners Encontech B.V., ISPT, Dow Benelux B.V. and Shell Global Solutions International B.V. for their support and contribution. All the suggestions and discussions with Maxim Glushenkov and Alexander Kronberg were very helpful. The great interest of Dow and Shell in this scientific work and their many suggestions were also much appreciated. Special thanks to Shell for quickly providing the xenon gas. This work has received co-funding with subsidy from the Topsector Energy by the Ministry of Economic Affairs and Climate Policy in the Netherlands (project number TEEI118005).

Appendix A. Supplementary material

Supplementary material related to this article can be found online at https://doi.org/10.1016/j.ces.2023.119554.

References

Aghsaee, M., Nativel, D., Bozkurt, M., Fikri, M., Chaumeix, N., Schulz, C., 2015. Experimental study of the kinetics of ethanol pyrolysis and oxidation behind reflected shock waves and in laminar flames. Proc. Combust. Inst. 35 (1), 393–400. https://doi.org/10.1016/J.PROCI.2014.05.063.

Barnes, R.W., Pratt, G.L., Wood, S.W., 1989. Pressure dependence of methane dissociation. J. Chem. Soc. Faraday Trans. 85 (3), 229–238.

Baulch, D.L., Pilling, M.J., Cobos, C.J., Cox, R.A., Esser, C., Frank, P., Just, T., Kerr, J.A., Troe, J., Walker, R.W., Warnatz, J., 1992. Evaluated kinetic data for combustion modelling. J. Phys. Chem. Ref. Data 21 (3), 411–734. https://doi.org/10.1063/1.555908.

Callear, A., 1983. Chapter 4 basic rrkm theory. In: Bamford, C., Tipper, C. (Eds.), Modern Methods in Kinetics. In: Comprehensive Chemical Kinetics, vol. 24. Elsevier, pp. 333–356. https://www.sciencedirect.com/science/article/pii/S0069804008702061.

Choudhary, R., Boddapati, V., Clees, S., Girard, J.J., Peng, Y., Shao, J., Davidson, D.F., Hanson, R.K., 2021. Shock tube study of ethanol pyrolysis II: rate constant measurements and modeling. Combust. Flame 233, 111554. https://doi.org/10.1016/j.combustflame.2021.111554.

Ezdin, B., Vasiljev, S., Yatsenko, D., Fedorov, V., Ivanova, M., Kalyada, V., Pakharukov, Y., Shabiev, F., Zarvin, A., 2023. Synthesis of carbon nanoparticles in a compression reactor in atmosphere of buffer gases. Tech. Phys. https://doi.org/10.1134/S1063784223010024.

Ezdin, B.S., Vasiljev, S.A., Yatsenko, D.A., Fedorov, V.E., Ivanova, M.N., Kalyada, V.V., Pakharukov, Y.V., Shabiev, F.K., Zarvin, A.E., 2022. The synthesis of carbon nanoparticles in a compression reactor in the atmosphere of buffer gases. Sib. J. Phys. 17 (3), 29–46. https://doi.org/10.25205/2541-9447-2022-17-3-29-46.

Golden, D.M., 2008. Yet another look at the reaction CH3 + H + M = CH4 + M. Int. J. Chem. Kinet. 40 (6), 310–319. https://doi.org/10.1002/KIN.20322. https://onlinelibrary.wiley.com/doi/full/10.1002/kin.20322. https://onlinelibrary.wiley.com/doi/abs/10.1002/kin.20322.

Hidaka, Y., Sato, K., Henmi, Y., Tanaka, H., Inami, K., 1999. Shock-tube and modeling study of methane pyrolysis and oxidation. Combust. Flame 118 (3), 340–358. https://doi.org/10.1016/S0010-2180(99)00010-3.

Jasper, A.W., Miller, J.A., 2009. Collisional Energy Transfer in Unimolecular Reactions: Direct Classical Trajectories for CH 4 <-> CH 3 + H in Helium, pp. 5612–5619.

Jasper, A.W., Miller, J.A., 2011. Theoretical unimolecular kinetics for CH 4 + M <-> CH 3 + H + M in eight baths, M = He, Ne, Ar, Kr, H 2, N 2, CO, and CH 4. J. Phys. Chem. 115 (24), 6438–6455. https://doi.org/10.1021/jp200048n. https://pubs.acs.org/doi/10.1021/jp200048n.

Kiecherer, J., Bänsch, C., Bentz, T., Olzmann, M., 2015. Pyrolysis of ethanol: a shock-tube/TOF-MS and modeling study. Proc. Combust. Inst. 35 (1), 465–472. https://doi.org/10.1016/J.PROCI.2014.05.086.

Kolbanovskij, Y., Shchipachev, V., Chernyak, N., Chernyshova, A., Grigoriev, A., 1982. Impulsnoe sgatie gasov v chimii i technologii (Pulsed compression of gases in chemistry and technology). Nauka, Moskow.

Kunz, O., Wagner, W., 2012. The GERG-2008 wide-range equation of state for natural gases and other mixtures: an expansion of GERG-2004. J. Chem. Eng. Data 57 (11), 3032–3091. https://doi.org/10.1021/je300655b.

Lemmon, E.W., Span, R., 2006. Short fundamental equations of state for 20 industrial fluids. J. Chem. Eng. Data 51 (3), 785–850. https://doi.org/10.1021/je050186n.

Matsugi, A., 2019. Origin of bath gas dependence in unimolecular reaction rates. J. Phys. Chem. A 123 (4), 764–770. https://doi.org/10.1021/acs.jpca.8b11081.

Nativel, D., Shu, B., Herzler, J., Fikri, M., Schulz, C., 2019. Shock-tube study of methane pyrolysis in the context of energy-storage processes. Proc. Combust. Inst. 37 (1), 197–204. https://doi.org/10.1016/J.PROCI.2018.06.083.

Schwaab, M., Lemos, L.P., Pinto, J.C., 2008. Optimum reference temperature for reparameterization of the Arrhenius equation. Part 2: problems involving multiple reparameterizations. Chem. Eng. Sci. 63 (11), 2895–2906. https://doi.org/10.1016/j.ces.2008.03.010.

Slotboom, Y., Kersten, S.R.A., 2023. Mapping of operating windows for methane and ethane pyrolysis in the pulsed compression reactor by experiments and modelling. Chem. Eng. J. 468, 143522. https://doi.org/10.1016/j.cej.2023.143522.

Slotboom, Y., Roosjen, S., Kronberg, A., Glushenkov, M., Kersten, S.R.A., 2021. Methane to ethylene by pulsed compression. Chem. Eng. J. 414, 128821. https://doi.org/10.1016/J.CEJ.2021.128821.

Span, R., Wagner, W., 2003. Equations of state for technical applications. II. Results for nonpolar fluids. Int. J. Thermophys. 24 (1), 41–109. https://doi.org/10.1023/A:1022310214958.

Troe, J., Ushakov, V.G., 2012. The dissociation/recombination reaction CH4 (+M) <->CH3 + H (+M): a case study for unimolecular rate theory. J. Chem. Phys. 136 (21), 214309. https://doi.org/10.1063/1.4717706. https://aip-scitation-org.ezproxy2.utwente.nl/doi/abs/10.1063/1.4717706.